# New description of the doublet bands in doubly odd nuclei

**Ganev, H. G.; Georgieva, A. I.; Brant, Slobodan; Ventura, A.**

# New description of the doublet bands in doubly odd nuclei

H. G. Ganev,[1] A. I. Georgieva,[1] S. Brant,[2] and A. Ventura[3]
[1]*Institute of Nuclear Research and Nuclear Energy, Bulgarian Academy of Sciences, Sofia 1784, Bulgaria*
[2]*Department of Physics, Faculty of Science, University of Zagreb, 10000 Zagreb, Croatia*
[3]*Ente per le Nuove tecnologie, l'Energia e l'Ambiente, I-40129 Bologna and Istituto Nazionale di Fisica Nucleare, Sezione di Bologna, Italy*
(Received 25 December 2008; published 28 April 2009)

The experimentally observed $\Delta I = 1$ doublet bands in some odd-odd nuclei are analyzed within the orthosymplectic extension of the interacting vector boson model (IVBM). A new, purely collective interpretation of these bands is given on the basis of the obtained boson-fermion dynamical symmetry of the model. It is illustrated by its application to three odd-odd nuclei from the $A \sim 130$ region, namely $^{126}$Pr, $^{134}$Pr, and $^{132}$La. The theoretical predictions for the energy levels of the doublet bands as well as $E2$ and $M1$ transition probabilities between the states of the yrast band in the last two nuclei are compared with experiment and the results of other theoretical approaches. The obtained results reveal the applicability of the orthosymplectic extension of the IVBM.

DOI: 10.1103/PhysRevC.79.044322 PACS number(s): 21.10.Re, 23.20.Lv, 21.60.Fw, 27.60.+j

## I. INTRODUCTION

In recent years, extensive experimental evidence for the existence of distinct band structures in odd-odd nuclei has been obtained. It has created an opportunity for testing the predictions of different theoretical models on the level properties of these nuclei. One such study involves the observation of doublet $\Delta I = 1$ bands in odd-odd $N = 75$ and $N = 73$ isotones in the $A \sim 130$ region. A large number of experimental data [1–8] have been accumulated in this mass region, showing that the yrast and yrare states with the $\pi h_{11/2} \otimes \nu h_{11/2}$ configuration form $\Delta I = 1$ doublet bands that are nearly degenerate in energy. They are built on the single-particle states of a valence neutron and a valence proton in the same unique-parity orbital $0h_{11/2}$. Pairs of bands have been found also in the $A \sim 105$ and $A \sim 190$ mass regions. Initially, these $\Delta I = 1$ doublet bands had been interpreted as a manifestation of "chirality" in the sense of the angular-momentum coupling [9]. Several theoretical models have been applied in a number of articles, like the tilted axis cranking (TAC) model [8,10–12], the core-quasiparticle coupling model [13], the particle-rotor model (PRM) [4,14,15], two quasiparticle+triaxial rotor model (TQPTR) [16], and the core-particle-hole coupling model (CPHCM) [6]. All these models have one assumption in common, they suppose a rigid triaxial core and hence support the interpretation of the doublet bands of chiral structure. On the contrary, all odd-odd nuclei in which twin bands have been observed have a different characteristic in common: They are in regions where even-even nuclei are $\gamma$-soft, i.e., effectively triaxial but not rigid. Their potential energy surface is rather flat in the $\gamma$ direction and the couplings with other core structures, not only the ground state band, are significant. It is evident that odd-odd nuclei in these mass regions do not satisfy all the requirements for the existence of chirality, but they can approach some of them or at least retain some fingerprints of chirality.

Many of the recent experiments and theoretical analysis do not support completely the chiral interpretation [17–21]. In particular, in an ideal situation, i.e., perfectly orthogonal angular-momentum vectors and stable triaxial nuclear shape, a perfect degeneracy between the identical spin states should be observed. In fact, the attainment of degeneracy is one of the key characteristics of chirality. This feature has not been observed in any of the chiral structures identified to date. Moreover, states with different quantum numbers in two nonchiral bands can also show an accidental degeneracy. Thus, one of the important tests of chirality is that the degenerate states in the two bands should also have similar physical properties, such as moment of inertia, quasiparticle alignments, transition quadrupole moments, and the related $B(E2)$ values for intraband $E2$ transitions. Some experimental studies have shown that the two bands have different shapes due to the different kinematical moments of inertia, which suggest a shape coexistence (triaxial and axial shapes). This is an interesting observation because the quantal nature of chirality automatically demands that a chiral partner band should have identical properties to the yrast triaxial rotational band. Similarly, it was also found that the experimental data for the behavior of other observables [equal $E2$ transitions, staggering behavior of the $M1$ values, the smoothness of the signature $S(I)$, etc.] do not support such a chiral structure [17–21]. These results demand a deeper and more detailed discussion of our understanding of the origin of doublet bands.

Within the framework of pair truncated shell model it was pointed out that the band structure of the doublet bands can be explained by the chopsticks-like motion of two angular momenta of the odd neutron and the odd proton [22–24]. It was found that the level scheme of $\Delta I = 1$ doublet bands arises not from the chiral structure but from different angular momentum configurations of the unpaired neutron and unpaired proton in the $0h_{11/2}$ orbitals, weakly coupled with the collective excitations of the even-even core. The same interpretation was given also in the quadrupole coupling model [25,26].

An alternative interpretation has been based on the interacting boson fermion-fermion model (IBFFM) [27,28], where

 

the energy degeneracy is obtained but a different nature is attributed to the two bands. A detailed analysis of the wave functions in IBFFM showed as well that the presence of configurations with the angular momenta of the proton, neutron, and core in the chirality favorable, almost orthogonal geometry, is substantial but far from being dominant. The large fluctuations of the deformation parameters $\beta$ and $\gamma$ around the triaxial equilibrium shape enhance the content of achiral configurations in the wave functions. The $\beta$ distribution of the yrast band has its maximum at larger deformations than that of the sideband. At higher angular momenta, this difference becomes very pronounced. In addition, the fluctuations of $\beta$ in the sideband become very large with increasing spin. In both bands the fluctuations of $\gamma$ increase with spin, being more pronounced in the sideband [29]. The composition of the yrast band, in terms of contributions from core states, shows that the yrast band is basically built on the ground state band of the even-even core. With increasing spin the admixture of the $\gamma$ band of the core becomes more pronounced. The sideband wave functions contain large components of the $\gamma$ band and with increasing spin, of higher-lying collective structures of the core, which near the band crossing become dominant. So, the conclusion of Refs. [20,29] was that the existence of twin bands in $^{134}$Pr should be attributed to a weak dynamic (fluctuation dominated) chirality combined with an intrinsic symmetry yet to be revealed. The IBFFM was applied to the doublet bands in $^{134}$Pr [17,20,29]. The $B(E2)$ values of the transitions depopulating the analog states are different from the chiral predictions and the $B(M1)$ staggering is not present [30]. The IBFFM was also applied for the description of the yrast $\pi h_{11/2} \otimes \nu h_{11/2}$ band in $^{126}$Pr [31].

The above variety of models and approaches dealing with the description of the doublet bands in odd-odd nuclei motivated us to consider their properties in the framework of the boson-fermion extension of the symplectic IVBM [32].

In the present work we carry out an analysis of the doublet bands in some doubly odd nuclei from the $A \sim 130$ region within the orthosymplectic extension [33] of the IVBM. The latter was proposed to encompass the treatment of the odd-mass nuclei. Further, the new version of IVBM was applied for the description of the ground and first excited positive and/or negative bands of odd-odd nuclei [34]. The spectrum of the positive-parity states in the odd-odd nuclei considered in this article is based on the odd proton and odd neutron (not necessary considered as proton particle-like and neutron holelike) that occupy the same single-particle level $h_{11/2}$. The theoretical description of the doubly odd nuclei under consideration is fully consistent and starts with the calculation of theirs even-even and odd-even neighbors. We consider the simplest physical picture in which two particles (or quasiparticles) with intrinsic spins taking a single $j$ value are coupled to an even-even core nucleus whose states belong to an $Sp^B(12, R)$ irreducible representation. Thus, the bands of the odd-mass and odd-odd nuclei arise as collective bands build on a given even-even nucleus. Therefore, within the framework of the orthosymplectic extension of the model a purely collective structure of the doublet bands is obtained.

The level structure of $^{126}$Pr, $^{134}$Pr, and $^{132}$La is analyzed in the framework of the orthosymplectic extension of the IVBM [33]. Thus to describe the structure of odd-odd nuclei, first a description of the appropriate even-even cores should be obtained.

The application of the theory to real nuclear systems is related to the fitting of the model parameters to the experimental data. The set of five parameters evaluated for the reproduction of the energies of different collective bands of the even-even core nuclei is further used with addition of only three new parameters in the calculations of the energy levels of the neighboring odd-$A$ and odd-odd nuclei. At the same time the number of described states is substantially increased in respect to the ones of the initial even-even cores, which is illustrated in the applications. That is why the correct choice of the collective states of the initial even-even nuclei, from which the basic model parameters are determined, is very important.

## II. THE EVEN-EVEN CORE NUCLEI

The algebraic structure of the IVBM is realized in terms of creation and annihilation operators $u_m^+(\alpha)$, $u_m(\alpha)$ $(m = 0, \pm 1)$. The bilinear products of the creation and annihilation operators of the two vector bosons generate the boson representations of the noncompact symplectic group $\mathrm{Sp}^B(12, R)$ [35]:

$$F_M^L(\alpha, \beta) = \sum_{k,m} C_{1k1m}^{LM} u_k^+(\alpha) u_m^+(\beta),$$
$$G_M^L(\alpha, \beta) = \sum_{k,m} C_{1k1m}^{LM} u_k(\alpha) u_m(\beta), \quad (1)$$
$$A_M^L(\alpha, \beta) = \sum_{k,m} C_{1k1m}^{LM} u_k^+(\alpha) u_m(\beta), \quad (2)$$

where $C_{1k1m}^{LM}$, which are the usual Clebsch-Gordan coefficients for $L = 0, 1, 2$ and $M = -L, -L+1, \ldots L$, define the transformation properties of Eqs. (1) and (2) under rotations. The commutation relations between the pair creation and annihilation operators (1) and the number preserving operators (2) are given in Ref. [35].

Being a noncompact group, the unitary representations of $\mathrm{Sp}^B(12, R)$ are of infinite dimension, which makes it impossible to diagonalize the most general Hamiltonian. When reduced to the group $\mathrm{U}^B(6)$, each irrep of the group $\mathrm{Sp}^B(12, R)$ decomposes into irreps of the subgroup characterized by the partitions [32,36]:

$$[N, 0^5]_6 \equiv [N]_6,$$

where $N = 0, 2, 4, \ldots$ (even irrep) or $N = 1, 3, 5, \ldots$ (odd irrep). The subspaces $[N]_6$ are finite dimensional, which simplifies the problem of diagonalization. Therefore the complete spectrum of the system can be calculated through the diagonalization of the Hamiltonian in the subspaces of all the unitary irreducible representations (UIR) of $\mathrm{U}^B(6)$, belonging to a given UIR of $\mathrm{Sp}^B(12, R)$, which further clarifies its role of a group of dynamical symmetry.

The Hamiltonian, corresponding to the unitary limit of IVBM [32]

$$\mathrm{Sp}^B(12,R) \supset \mathrm{U}^B(6) \supset \mathrm{U}^B(3) \otimes \mathrm{U}^B(2) \supset \mathrm{O}^B(3) \otimes [\mathrm{U}^B(1) \otimes \mathrm{U}^B(1)], \quad (3)$$

expressed in terms of the first- and second-order invariant operators of the different subgroups in the chain (3) is [32]:

$$H = aN + bN^2 + \alpha_3 T^2 + \beta_3 L^2 + \alpha_1 T_0^2. \quad (4)$$

Taking into account the relations $T = 2\lambda$ and $N = \lambda + 2\mu$ between the quantum numbers of the mutually complementary groups $\mathrm{SU}^B(3)$ and $\mathrm{U}^B(2)$ in Eq. (3), it becomes obvious that $H$ [Eq. (4)] is diagonal in the basis

$$|[N]_6; (\lambda,\mu); KLM; T_0\rangle \equiv |(N,T); KLM; T_0\rangle, \quad (5)$$

labeled by the quantum numbers of the subgroups of the chain (3). Its eigenvalues are the energies of the basis states of the boson representations of $\mathrm{Sp}^B(12,R)$:

$$E[(N,T),L,T_0] = aN + bN^2 + \alpha_3 T(T+1) + \beta_3 L(L+1) + \alpha_1 T_0^2. \quad (6)$$

The construction of the symplectic basis for the even IR of $\mathrm{Sp}^B(12,R)$ is given in detail in Ref. [32]. The $\mathrm{Sp}^B(12,R)$ classification scheme for the $\mathrm{SU}^B(3)$ boson representations for even value of the number of bosons $N$ is shown on Table I in Ref. [32] (see also Table I).

The most important application of the $\mathrm{U}^B(6) \subset \mathrm{Sp}^B(12,R)$ limit of the theory is the possibility it affords for describing both even- and odd-parity bands up to very high angular momentum [32]. To do this we first have to identify the experimentally observed bands with the sequences of basis states of the even $\mathrm{Sp}^B(12,R)$ irrep (Table I). As we deal with the symplectic extension we are able to consider all even eigenvalues of the number of vector bosons $N$ with the corresponding set of $T$-spins, which uniquely define the $\mathrm{SU}^B(3)$ irreps $(\lambda,\mu)$. The multiplicity index $K$ appearing in the final reduction to the $\mathrm{SO}^B(3)$ is related to the projection of $L$ on the body fixed frame and is used with the parity $(\pi)$ to label the different bands $(K^\pi)$ in the energy spectra of the nuclei. For the even-even nuclei we have defined the parity of the states as $\pi_{\mathrm{core}} = (-1)^T$ [32]. This allowed us to describe both positive and negative bands.

Further, we use the algebraic concept of "yrast" states, introduced in Ref. [32]. According to this concept we consider as yrast states the states with given $L$, that minimize the energy (6) with respect to the number of vector bosons $N$ that build them. Thus the states of the ground state band (GSB) were identified with the $\mathrm{SU}^B(3)$ multiplets $(0,\mu)$ [32]. In terms of $(N,T)$ this choice corresponds to $(N = 2\mu, T = 0)$ and the sequence of states with different numbers of bosons $N = 0, 4, 8, \ldots$ and $T = 0$, $T_0 = 0$. Hence the minimum values of the energies (6) are obtained at $N = 2L$.

The presented mapping of the experimental states onto the $\mathrm{SU}^B(3)$ basis states, using the algebraic notion of yrast states, is a particular case of the so called "stretched" states [37]. The latter are defined as the states with $(\lambda_0 + 2k, \mu_0)$ or $(\lambda_0, \mu_0 + k)$, where $N_i = \lambda_0 + 2\mu_0$ and $k = 0, 1, 2, 3, \ldots$. In the symplectic extension of the IVBM the change of the number $k$, which is related in the applications to the angular momentum $L$ of the states, gives rise to the collective bands. This is achieved by multiple action of one and the same of the pair rasing generators (1) that are used to define the transition operators [38]. For the GSB those are the minimum weight $\mathrm{SU}^B(3)$ states of a given $\mathrm{U}^B(6)$ representation, which further motivate their definition as yrast state.

It was established [39] that the correct placement of the bands in the spectrum strongly depends on their bandheads' configuration, and in particular, on the minimal or initial number of bosons, $N = N_i$, from which they are built. The latter determines the starting position of each excited band. In the present application we take for $N_i$ the value at which the best $\chi^2$ is obtained in the fitting procedure for the energies of the considered excited band.

TABLE I. Classification scheme of basis states (16) according the decompositions given by the chain (15).

| $N$ | $T$ | $(\lambda,\mu)$ | $K$ | $L$ | $J = L \pm I$ |
|---|---|---|---|---|---|
| 0 | 0 | (0, 0) | 0 | 0 | $I$ |
| 2 | 1 | (2, 0) | 0 | 0, 2 | $I; 2 \pm I$ |
| | 0 | (0, 1) | 0 | 1 | $1 \pm I$ |
| | 2 | (4, 0) | 0 | 0, 2, 4 | $I; 2 \pm I; 4 \pm I$ |
| 4 | 1 | (2, 1) | 1 | 1, 2, 3 | $1 \pm I; 2 \pm I; 3 \pm I$ |
| | 0 | (0, 2) | 0 | 0, 2 | $I; 2 \pm I$ |
| | 3 | (6, 0) | 0 | 0, 2, 4, 6 | $I; 2 \pm I; 4 \pm I; 6 \pm I$ |
| | 2 | (4, 1) | 1 | 1, 2, 3, 4, 5 | $1 \pm I; 2 \pm I; 3 \pm I; 4 \pm I; 5 \pm I$ |
| 6 | 1 | (2, 2) | 2 | 2, 3, 4 | $2 \pm I; 3 \pm I; 4 \pm I$ |
| | | | 0 | 0, 2 | $I; 2 \pm I$ |
| | 0 | (0, 3) | 0 | 1, 3 | $1 \pm I; 3 \pm I$ |
| | 4 | (8, 0) | 0 | 0, 2, 4, 6, 8 | $I; 2 \pm I; 4 \pm I; 6 \pm I; 8 \pm I$ |
| | 3 | (6, 1) | 1 | 1, 2, 3, 4, 5, 6, 7 | $1 \pm I; 2 \pm I; 3 \pm I; 4 \pm I; 5 \pm I; 6 \pm I; 7 \pm I; 8 \pm I$ |
| | 2 | (4, 2) | 2 | 2, 3, 4, 5, 6 | $2 \pm I; 3 \pm I; 4 \pm I; 5 \pm I; 6 \pm I$ |
| 8 | | | 0 | 0, 2, 4 | $I; 2 \pm I; 4 \pm I$ |
| | 1 | (2, 3) | 2 | 2, 3, 4, 5 | $2 \pm I; 3 \pm I; 4 \pm I; 5 \pm I$ |
| | | | 0 | 1, 3 | $1 \pm I; 3 \pm I$ |
| | 0 | (0, 4) | 0 | 0, 2, 4 | $I; 2 \pm I; 4 \pm I$ |
| ⋮ | ⋮ | ⋮ | ⋮ | ⋮ | ⋮ |

Thus, for the description of the different excited bands, we first determine the $N_i$ of the bandhead structure and develop the corresponding excited band over the stretched $SU^B(3)$ multiplets. This corresponds to the sequence of basis states with $N = N_i, N_i + 4, N_i + 8, \ldots (\Delta N = 4)$. The values of $T$ for the first type of stretched states ($\lambda$ changing) are changing by step $\Delta T = 2$, whereas for the second type ($\mu$ changing) $-T$ is fixed so that in both cases the parity is preserved even or odd, respectively. For all presented even-even nuclei, the states of the described excited bands are associated with the stretched states of the first type ($\lambda$ changing).

To describe the structure of odd-mass and odd-odd nuclei, first a description of the appropriate even-even cores should be obtained. We determine the values of the five phenomenological model parameters $a, b, \alpha_3, \beta_3, \alpha_1$ by fitting the energies of the ground and $\gamma$ bands of the even-even nuclei to the experimental data [40], using a $\chi^2$ procedure.

Numerous IBM studies of even-even nuclei in the $A \sim 130$ mass region have shown that these nuclei are well described by the O(6) symmetry of the IBM, that in the classical limit corresponds to the Wilets-Jean model of a $\gamma$-unstable rotor [41], and that the accepted interpretation is that they are $\gamma$-soft. The core nucleus $^{124}$Ce follows the systematic trend of the Ce isotopes. The heavier isotopes are $\gamma$-soft [O(6)-like in the IBM terminology], and the lighter ones are considerably deformed, but they never reach the rigid rotor structure that corresponds to the SU(3) limit of the IBM. The transition between these two structures occurs for $^{126}$Ce and is reflected in the dynamics of bands in the neighboring odd-even and odd-odd nuclei. In contrast to the O(6)-like spectra observed in the odd-odd isotopes $^{130,132}$Pr [42], the structure of $^{126}$Pr reflects the transitional SU(3)-O(6) nature of the core nucleus $^{124}$Ce.

Here, we must point out that only in the considered dynamical symmetry (3) of the IVBM, due to the employed "algebraic yrast" condition $N = 2L$ and the reduction rules connecting the values of the number of bosons $N$ with their angular momentum $L$ the energies of the collective states of ground state band [32], for example, can be written as:

$$E_g(L) = (2a - 4b)L + (4b + \beta_3)L(L + 1), \tag{7}$$

where obviously the rotational $L(L + 1)$ and vibrational $L$ collective modes are mixed and the type of collectivity depends on the ratio of the coefficients in front of these two terms. In analogy it could be shown that the two collective modes are mixed in the excited bands as well. Hence we can describe quite well in the same group chain of the symplectic extension, the even-even cores with various collective properties that need different dynamical symmetries or their mixture in the IBM.

The theoretical predictions for the even-even core nuclei are presented in Figs. 1–3. For comparison, the predictions of IBM and CPHCM are also shown. The IBM results for $^{124}$Ce and $^{134}$Ce are extracted from Refs. [17,31] and those of CPHCM for $^{132}$Ba from Ref. [6], respectively. From the figures one can see that the calculated energy levels of both ground state and $\gamma$ bands agree rather well up to high angular momenta with the observed data. Except for the GSB of $^{134}$Ce, for which the IVBM and IBM results are almost identical, the IVBM

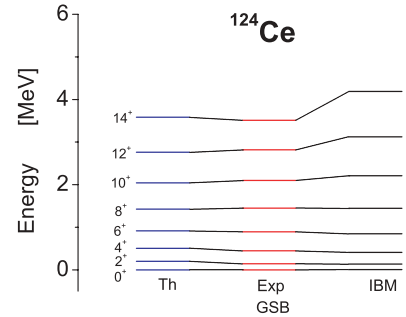


FIG. 1. (Color online) Comparison of the theoretical, experimental, and IBM energies for the ground band of $^{124}$Ce.

predictions reproduce better the band structures compared to CPHCM and IBM.

## III. FERMION DEGREES OF FREEDOM

To incorporate the intrinsic spin degrees of freedom into the symplectic IVBM, we extend the dynamical algebra of $Sp^B(12, R)$ to the orthosymplectic algebra of $OSp(2\Omega/12, R)$ [33]. For this purpose we introduce a particle (quasiparticle) with spin $j$ and consider a simple core plus particle picture. Thus, in addition to the boson collective degrees of freedom [described by dynamical symmetry group $Sp^B(12, R)$] we introduce creation and annihilation operators $a_m^\dagger$ and $a_m$ ($m = -j, \ldots, j$), which satisfy the anticommutation relations

$$\begin{aligned} \{a_m^\dagger, a_{m'}^\dagger\} &= \{a_m, a_{m'}\} = 0, \\ \{a_m, a_{m'}^\dagger\} &= \delta_{mm'}. \end{aligned} \tag{8}$$

All bilinear combinations of $a_m^+$ and $a_{m'}$, namely

$$f_{mm'} = a_m^\dagger a_{m'}^\dagger, \quad m \neq m' \tag{9}$$

$$g_{mm'} = a_m a_{m'}, \quad m \neq m';$$

$$C_{mm'} = (a_m^\dagger a_{m'} - a_{m'} a_m^\dagger)/2 \tag{10}$$

generate the (Lie) fermion pair algebra of $SO^F(2\Omega)$. Their commutation relations are given in Ref. [33]. The number preserving operators (10) generate maximal compact subalgebra $U^F(\Omega)$ of $SO^F(2\Omega)$. The upper script $B$ or $F$ denotes the boson or fermion degrees of freedom, respectively.

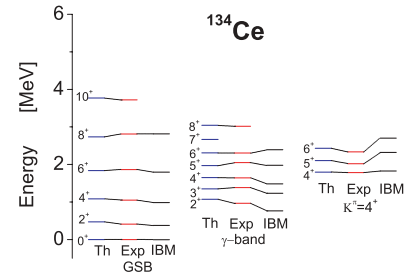


FIG. 2. (Color online) Comparison of the theoretical, experimental, and IBM energies for the ground and first excited $\gamma$ and $K^\pi = 4^+$ bands of $^{134}$Ce.

### A. Fermion dynamical symmetries

As can be seen from Eq. (10), the full number conserving symmetry of a fermion of spin $j$ is $\mathrm{U}^F(2j+1)$. In general, the full dynamical algebra build from all bilinear combinations [Eqs. (9) and (10)] of creation and annihilation fermion operators is the $\mathrm{SO}^F(2\Omega)$ algebra [for a multilevel case $\Omega = \sum_j (2j+1)$]. One can further construct a certain fermion dynamical symmetry, i.e., the group-subgroup chain:

$$\mathrm{SO}^F(2\Omega) \supset G' \supset G'' \supset \ldots . \tag{11}$$

In particular for one particle occupying a single level $j$ we are interested in the following dynamical symmetry:

$$\mathrm{SO}^F(2\Omega) \supset \mathrm{Sp}(2j+1) \supset \mathrm{SU}^F(2), \tag{12}$$

where $\mathrm{Sp}(2j+1)$ is the compact symplectic group. The dynamical symmetry (12) remains valid also for the case of two particles occupying the same level $j$. In this case, the allowed values of the quantum number $I$ of $\mathrm{SU}^F(2)$ in Eq. (12) according to reduction rules are $I = 0, 2, \ldots, 2j-1$ [43]. If the two particles occupy different levels $j_1$ and $j_2$ of the same or different major shell(s), one can consider the chain

$$\mathrm{SO}^F(2\Omega) \supset \mathrm{U}^F(\Omega) \begin{array}{c} \nearrow \mathrm{U}^F(\Omega_1) \supset \mathrm{Sp}(2j_1+1) \supset \mathrm{SU}^F_{I_1}(2) \searrow \\ \searrow \mathrm{U}^F(\Omega_2) \supset \mathrm{Sp}(2j_2+1) \supset \mathrm{SU}^F_{I_2}(2) \nearrow \end{array} \mathrm{SU}^F(2), \tag{13}$$

where $\Omega = \Omega_1 + \Omega_2$. We want to point out that although the final group $\mathrm{SU}^F(2)$ that appears in the chain (13) is the same as in Eq. (12), its content is different. Here the values of the common fermion angular momentum $I$ are determined by the vector sum of the two individual spins $I_1$ and $I_2$, respectively. Nevertheless, for simplicity hereafter we will use just the reduction $\mathrm{SO}^F(2\Omega) \supset \mathrm{SU}^F(2)$ [i.e., dropping all intermediate subgroups between $\mathrm{SO}^F(2\Omega)$ and $\mathrm{SU}^F(2)$] and keep in mind the proper content of the set of $I$ values for one- and/or two-particle cases, respectively. We consider only the highest weight states of $\mathrm{Sp}(2j+1)$ with $\upsilon = n = 1$ (odd-mass nuclei) and $\upsilon = n = 2$ (odd-odd nuclei) that are multiplicity free [43,44]. $\upsilon$ is the quantum number of the $\mathrm{Sp}(2j+1)$ algebra and $n$ is the number of fermions. Thus, no multiplicity indices are required in the latter reduction.

### B. Bose-Fermi symmetry

Once the fermion dynamical symmetry is determined we proceed with the construction of the Bose-Fermi symmetries. If a fermion is coupled to a boson system having itself a dynamical symmetry (e.g., such as an IBM core), the full symmetry of the combined system is $G^B \otimes G^F$. Bose-Fermi symmetries occur if at some point the same group appears in both chains

$$G^B \otimes G^F \supset G^{\mathrm{BF}}, \tag{14}$$

i.e., the two subgroup chains merge into one. It should be noted that (14) is true only for the diagonal subgroup $G^B \otimes G^F$, i.e., the one in which the two group elements multiplied directly are parametrized by the same parameters. In this way the Bose-Fermi symmetry not only constrains parameters by the choice of particular subgroup chains in the boson and fermion sectors but also specifies the interaction between the two.

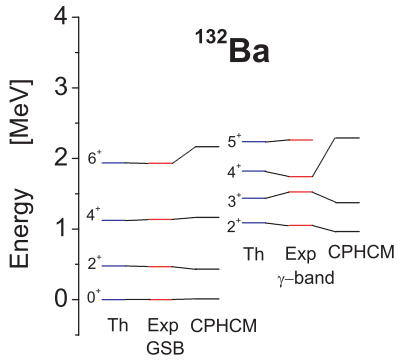


FIG. 3. (Color online) Comparison of the theoretical, experimental, and CPHCM energies for the ground and $\gamma$ bands of $^{132}$Ba.

## IV. DYNAMICAL SUPERSYMMETRY

The standard approach to supersymmetry in nuclei (dynamical supersymmetry) is to embed the Bose-Fermi subgroup chain of $G^B \otimes G^F$ into a larger supergroup G, i.e., $G \supset G^B \otimes G^F$. It is our intention in this article to do that for chains describing odd-odd nuclei.

Making use of the embedding $\mathrm{SU}^F(2) \subset \mathrm{SO}^F(2\Omega)$ and considerations from the preceding section, we make orthosymplectic (supersymmetric) extension of the IVBM that is defined through the chain [33]:

$$\begin{array}{lll} O\,\mathrm{Sp}(2\Omega/12, R) \supset & \mathrm{SO}^F(2\Omega) \otimes & \mathrm{Sp}^B(12, R) \\ & & \Downarrow \\ & \Downarrow \quad \otimes & \mathrm{U}^B(6) \\ & & N \\ & & \Downarrow \\ & \mathrm{SU}^F(2) \quad \otimes & \mathrm{SU}^B(3) \otimes \mathrm{U}^B_T(2) \\ & I \qquad\quad & (\lambda, \mu) \Longleftrightarrow (N, T) \\ & \quad \searrow \quad & \Downarrow \\ & & \otimes \ \mathrm{SO}^B(3) \otimes \mathrm{U}^B(1) \\ & & L \qquad\quad T_0 \\ & & \Downarrow \\ & \mathrm{Spin}^{\mathrm{BF}}(3) \supset & \mathrm{Spin}^{\mathrm{BF}}(2), \\ & J \qquad\quad & J_0 \end{array} \tag{15}$$

where below the different subgroups the quantum numbers characterizing their irreducible representations are given. $\mathrm{Spin}^{\mathrm{BF}}(n)$ $(n = 2, 3)$ denotes the universal covering group of $\mathrm{SO}(n)$.

In the next section we present the application of the boson-fermion extension of IVBM, developed for the description of the collective bands of even-even [32] and odd-mass [33] nuclei, to include in our considerations the positive-parity states of the yrast and sidebands of odd-odd nuclei from $A \sim 130$ region, build on $\pi h_{11/2} \otimes \nu h_{11/2}$ configuration.

## V. THE ENERGY SPECTRA OF ODD-MASS AND ODD-ODD NUCLEI

We can label the basis states according to the chain (15) as:

$$|[N]_6; (\lambda, \mu); K L; I; J J_0; T_0\rangle \equiv |[N]_6; (N, T); K L; I; J J_0; T_0\rangle, \tag{16}$$

where $[N]_6$, the $\mathrm{U}^B(6)$ labeling quantum number, and $(\lambda, \mu)$, the $\mathrm{SU}^B(3)$ quantum numbers, characterize the core excitations; $K$ is the multiplicity index in the reduction $\mathrm{SU}^B(3) \supset \mathrm{SO}^B(3)$, $L$ is the core angular momentum, $I$ is the intrinsic spin of an odd particle (or the common spin of two fermion particles for the case of odd-odd nuclei), $J$, $J_0$ are the total (coupled boson-fermion) angular momentum and its third projection, and $T$, $T_0$ are the $T$-spin and its third projection, respectively. Because the $\mathrm{SO}(2\Omega)$ label is irrelevant for our application, we drop it in the states (16).

The Hamiltonian of the combined boson-fermion system can be written as linear combination of the Casimir operators of the different subgroups in (15):

$$H = aN + bN^2 + \alpha_3 T^2 + \beta_3' L^2 + \alpha_1 T_0^2 + \eta I^2 + \gamma' J^2 + \zeta J_0^2 \tag{17}$$

and it is obviously diagonal in the basis (16) labeled by the quantum numbers of their representations. Then the eigenvalues of the Hamiltonian (17) that yield the spectrum of the odd-mass and odd-odd systems are:

$$E(N; T, T_0; L, I; J, J_0) = aN + bN^2 + \alpha_3 T(T+1) + \beta_3' L(L+1) + \alpha_1 T_0^2 + \eta I(I+1) + \gamma' J(J+1) + \zeta J_0^2. \tag{18}$$

We note that only the last three terms of Eq. (17) come from the orthosymplectic extension. We choose parameters $\beta_3' = \frac{1}{2}\beta_3$ and $\gamma' = \frac{1}{2}\gamma$ instead of $\beta_3$ and $\gamma$ to obtain the Hamiltonian form of Ref. [32] (setting $\beta_3 = \gamma$), when for the case $I = 0$ (hence $J = L$) we recover the symplectic structure of the IVBM.

The infinite set of basis states classified according to the reduction chain (15) are schematically shown in Table I. The fourth and fifth columns show the $\mathrm{SO}^B(3)$ content of the $\mathrm{SU}^B(3)$ group, given by the standard Elliott's reduction rules [45], while in the next column are given the possible values of the common angular momentum $J$, obtained by coupling of the orbital momentum $L$ with the spin $I$. The latter is vector coupling and hence all possible values of the total angular momentum $J$ should be considered. For simplicity, only the maximally aligned $(J = L + I)$ and maximally antialigned $(J = L - I)$ states are illustrated in Table I.

The basis states (16) can be considered as a result of the coupling of the orbital $|(N, T); K L M; T_0\rangle$ (5) and spin $\phi_{j\equiv I,m}$ wave functions. Then, if the parity of the single particle is $\pi_{\mathrm{sp}}$, the parity of the collective states of the odd-$A$ nuclei will be $\pi = \pi_{\mathrm{core}}\pi_{\mathrm{sp}}$ [33]. In analogy, one can write $\pi = \pi_{\mathrm{core}}\pi_{\mathrm{sp}}(1)\pi_{\mathrm{sp}}(2)$ for the case of odd-odd nuclei. Thus, the description of the positive- and/or negative-parity bands requires only the proper choice of the core bandheads, on which the corresponding single particle(s) is (are) coupled to, generating in this way the different odd-$A$ (odd-odd) collective bands.

Further in the present considerations, the "yrast" conditions yield relations between the number of bosons $N$ and the coupled angular momentum $J$ that characterizes each collective state. For example, the collective states of the GSB $K_J^\pi = \frac{5}{2}^+$ ($^{125}$Ce) of the odd-mass nuclei are identified with the $\mathrm{SU}^B(3)$ multiplets $(0, \mu)$ that yield the sequence $N = 2(J - I) = 0, 2, 4, \ldots$ for the corresponding values $J = \frac{5}{2}, \frac{7}{2}, \frac{9}{2}, \ldots$. The $T$-spin for the $\mathrm{SU}^B(3)$ multiplets $(0, \mu)$ is $T = 0$ and hence $\pi_{\mathrm{core}} = (-1)^T = (+)$. Here it is assumed that the single particle has $j \equiv I = 5/2$ and parity $\pi_{\mathrm{sp}} = (+)$, so the common parity $\pi$ is also positive.

For the description of the different excited bands, we first determine the $N_i$ of the bandhead structure and then we map the states of the corresponding band onto the sequence of basis states with $N = N_i, N_i + 2, N_i + 4, \ldots$ $(\Delta N = 2)$ and $T =$ even $=$ fixed or $T =$ odd $=$ fixed, respectively. This choice corresponds to the stretched states of the second type ($\mu$ changing). In general, except for the excited bands of the even-even nuclei for which the stretched states of the first type ($\lambda$ changing) are used, the stretched states of the second type ($\mu$ changing) are considered in all the calculations of the collective states of the odd-mass and doubly odd nuclei.

The number of adjustable parameters needed for the complete description of the collective spectra of both odd-$A$ and odd-odd nuclei is three, namely $\gamma$, $\zeta$, and $\eta$. The first two are evaluated by a fit to the experimental data [40] of the GSB of the corresponding odd-$A$ neighbor, while the last one is introduced in the final step of the fitting procedure for the odd-odd nucleus, respectively. For the $A \sim 130$ region where the doublet bands are built on $\pi h_{11/2} \otimes \nu h_{11/2}$ configuration, the two fermions occupy the same single-particle level $j_1 = j_2 = j = 11/2$ with negative parity $(\pi_{\mathrm{sp}} = -)$ and the fermion reduction chain (12) can be used.

The odd-$A$ neighboring nuclei $^{125}$Ce and $^{135}$Ce can be considered as a neutron coupled to the even-even cores $^{124}$Ce and $^{134}$Ce, while the $^{133}$La can be considered as a proton coupled to the $^{132}$Ba, respectively. The low-lying positive-parity states of the GSB in odd-$A$ neighbors are based on positive-parity proton and positive-parity neutron configurations $(s_{\frac{1}{2}}, d_{\frac{3}{2}}, d_{\frac{5}{2}}, g_{\frac{7}{2}})$, whereas those of negative parity are based on $h_{11/2}$. For each nucleus under consideration we take into account only the first available single-particle orbit $j_1$ [generating the groups $\mathrm{SO}(2\Omega_1)$ and/or $\mathrm{U}(\Omega_1)$ with $\Omega_1 = (2j_1 + 1)$]. Thus, in the present calculations only the single-particle levels $j = 5/2$ ($^{125}$Ce) and $j = 11/2$ ($^{135}$Ce,

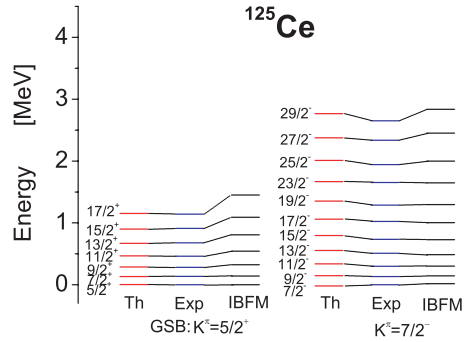


FIG. 4. (Color online) Comparison of the theoretical, experimental, and IBFM energies for the ground $K^\pi_J = \frac{5}{2}^+$ and first excited $K^\pi_J = \frac{7}{2}^-$ bands of $^{125}$Ce.

$^{133}$La), respectively, are considered. We want to point out that for the description of the excited bands (e.g., $K^\pi_J = 7/2^-$ of $^{125}$Ce, $K^\pi_J = 19/2^+$ of $^{135}$Ce) with opposite parity additional single-particle levels are not involved. The collective states of the odd-$A$ (or odd-odd) system are built on the proper SU$^B$(3) multiplets $(\lambda, \mu)$ so that the common positive- or negative-parity $\pi = \pi_{\rm core}\pi_{\rm sp}$ is correctly reproduced. For example, the $K^\pi_J = 7/2^-$ band of $^{125}$Ce is obtained by the coupling of a particle with $j = 5/2$ ($\pi_{\rm sp} = +$) to the core SU$^B$(3) multiplets $(18, \mu)$ ($\mu$ changing) ($T = 9$ and hence $\pi_{\rm core} = -$) so that the common parity is negative.

The comparison between the experimental spectra for the GSB and first excited band using the values of the model parameters given in Table II for the nuclei $^{125}$Ce, $^{135}$Ce, and $^{133}$La is illustrated in Figs. 4–6. One can see from the figures that the calculated energy levels agree rather well in general with the experimental data up to very high angular momenta. For comparison, in Figs. 4 and 6 the IBFM and CPHCM results for $^{125}$Ce and $^{133}$La are also shown. They are extracted from Refs. [31] and [6], respectively.

For the calculation of the odd-odd nuclei spectra a second particle should be coupled to the core. In our calculations a consistent procedure is employed that includes the analysis of the even-even and odd-even neighbors of the nucleus under consideration. Thus, as a first step an odd particle was coupled to the boson core to obtain the spectra of the odd-mass neighbors $^{125}$Ce, $^{135}$Ce, and $^{133}$La. As a second step, we consider an addition of a second particle to the boson-fermion system.

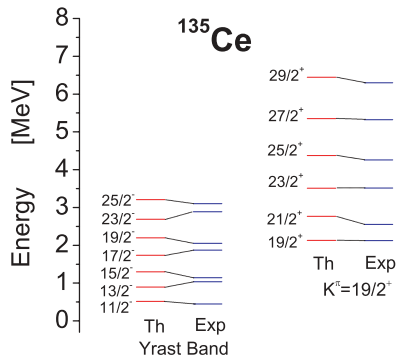


FIG. 5. (Color online) Comparison of the theoretical and experimental energies for the yrast $K^\pi_J = \frac{11}{2}^-$ and first excited $K^\pi_J = \frac{19}{2}^+$ bands of $^{135}$Ce.

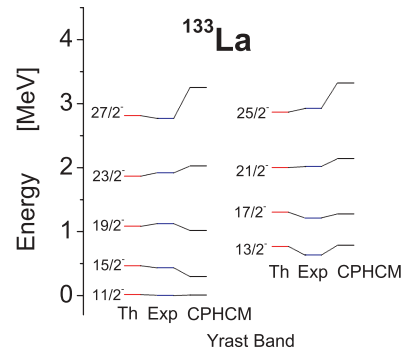


FIG. 6. (Color online) Comparison of the theoretical, experimental, and CPHCM energies for the yrast $K^\pi_J = \frac{11}{2}^-$ band of $^{133}$La.

TABLE II. Values of the model parameters.

| Nucl. | Bands | $N_i$ $T$ $T_0$ $J$ | $\chi^2$ | Parameters |
|---|---|---|---|---|
| | | | | $a = 0.02855$ |
| | Yrast: | | | |
| $^{126}$Pr | | 24 0 0 | $L + I$ 0.0017 | $b = -0.00120$ |
| | $K^\pi = 8^+$ | | | |
| | | | | $\alpha_3 = 0.00680$ |
| | | | | $\beta_3 = 0.01774$ |
| $I = 8$ | | | | |
| | | | | $\alpha_1 = 0.01387$ |
| | | | | $\eta = -0.00906$ |
| | | | | $\gamma = 0.01691$ |
| | | | | $\zeta = -0.01132$ |
| | | | | $a = 0.07449$ |
| | Yrast | | | |
| $^{132}$La | | 44 0 0 | $L - I$ 0.0034 | $b = 0.00690$ |
| | $K^\pi = 8^+$ | | | |
| | | | | $\alpha_3 = 0.05709$ |
| | Side | | | $\beta_3 = 0.04847$ |
| $I = 8$ | | 50 2 0 | $L - I$ 0.0088 | |
| | $K^\pi = 11^+$ | | | $\alpha_1 = 0.06076$ |
| | | | | $\eta = 0.02360$ |
| | | | | $\gamma = 0.04796$ |
| | | | | $\zeta = 0.02960$ |
| | | | | $a = 0.08190$ |
| | Yrast: | | | |
| $^{134}$Pr | | 10 0 0 | $L + I$ 0.0046 | $b = 0.00473$ |
| | $K^\pi = 8^+$ | | | |
| | | | | $\alpha_3 = 0.03637$ |
| | Side: | | | $\beta_3 = 0.03660$ |
| $I = 8$ | | 14 4 0 | $L + I$ 0.0020 | |
| | $K^\pi = 8^+$ | | | $\alpha_1 = 0.04424$ |
| | | | | $\eta = -0.01876$ |
| | | | | $\gamma = 0.03002$ |
| | | | | $\zeta = 0.00061$ |

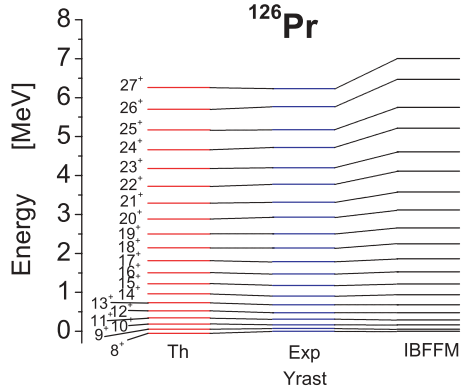


FIG. 7. (Color online) Comparison of the theoretical, experimental, and IBFFM energies for 20 levels of the yrast band of $^{126}$Pr.

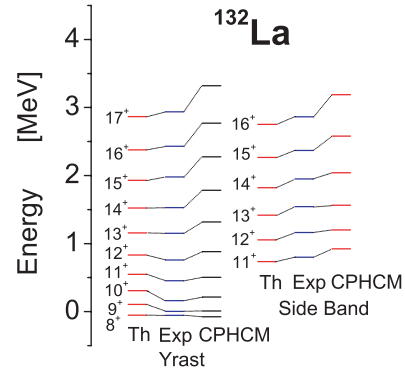


FIG. 9. (Color online) Comparison of the theoretical, experimental and CPHCM energies for 10 levels of the yrast and 6 levels of the sidebands $^{132}$La.

In our application, the most important point is the identification of the experimentally observed states with a certain subset of basis states from (ortho-)symplectic extension of the model. Here we consider a more general mapping when the states of the GSB of the odd-odd nuclei are associated with a sequence of $\mathrm{SU}^B(3)$ multiplets $(0, \mu)$ but the band starts with the multiplet $(0, \mu_0)$ instead of $(0, 0)$. Thus, to the states of the yrast band with $J = I, I + 1, I + 2, \ldots$ of the odd-odd nuclei we put into correspondence the $\mathrm{SU}^B(3)$ multiplets $(0, \mu)$ ($\mu$ changing) of the basis states (16) that in terms of $(N, T)$ correspond to $(N = 2\mu, T = 0)$ and the sequence of states with different numbers of bosons $N = N_0, N_0 + 2, N_0 + 4, \ldots$ ($\Delta N = 2$). The chosen set of $\mathrm{SU}^B(3)$ multiplets $(0, \mu)$ means that the GSB of the odd-odd as well as that of odd-mass nuclei is built on the GSB of the even-even core nucleus. We recall that in contrast to the IBM, the symplectic core structure [described by *different* $\mathrm{SU}^B(3)$ multiplets $(0, \mu)$] within the IVBM is active allowing the change of the number of bosons. The "yrast" condition that results from this mapping of the band's states over the stretched states $(\lambda_0 = 0, \mu_0 + k)$ yields $N = 2\mu_0 + 2L$ (or $k = L$). In particular, when the bandhead structure is determined by $N_0 = 0$ bosons, the yrast condition reduces to $N = 2L$ (or $\mu = L$) [32,33]. To visualize the correspondence under consideration, we illustrate the selected subset of basis states in Table III. Hence one obtains the observed ground state of the yrast band with $K^\pi_J = 8^+$ for $^{126}$Pr,$^{134}$Pr, and $^{132}$La nuclei simply attributing to it only the angular momentum $I = 8$ from the vector coupling of the proton $I_p = \frac{11}{2}$ and neutron $I_n = \frac{11}{2}$ momenta.

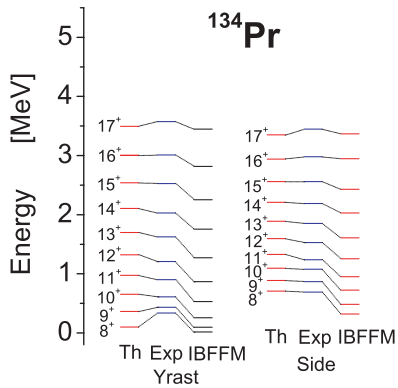


FIG. 8. (Color online) Comparison of the theoretical, experimental, and IBFFM energies for 10 levels of the yrast and 10 levels of the sidebands of $^{134}$Pr.

For the description of the side (yrare) band built also on the $\pi h_{11/2} \otimes \nu h_{11/2}$ configuration that can be considered an excited band, we first determine the collective structure of the bandhead $N_i = \lambda_0 + 2\mu_0$ and then map the states of this band onto the sequences of basis states with $N = N_i, N_i + 2, N_i + 4, \ldots$ ($\Delta N = 2$) and $T =$ even $=$ fixed. This choice corresponds to the stretched states of the second type ($\mu$ changing). The $\mathrm{SU}^B(3)$ multiplets $(\lambda \neq 0, \mu)$ attributed to the sideband suggest similar collective structure for this band compared to that of its "doublet partner." Similar interpretation of the two bands takes place in the IBFFM, where the yrast band is basically built on the GSB [described within *a single* SU(3) multiplet $(\lambda, \mu)$] of the even-even core, while the structure of the sideband is that of odd proton and odd neutron coupled to the $\gamma$ band of the core and in the high-spin region contains sizable components of the higher-lying core structures.

The theoretical predictions for the yrast and sidebands based on $\pi h_{11/2} \otimes \nu h_{11/2}$ configuration for the three odd-odd nuclei $^{126}$Pr, $^{134}$Pr, and $^{132}$La from $A \sim 130$ region are presented in Figs. 7, 8, and 9, respectively. For comparison, the IBFFM (Refs. [29,31]) and CPHCM (Ref. [6]) results are also shown. In Table II, the values of $N_i, T, T_0, J$, and $\chi^2$ for each band under consideration are also given. From the figures one can see the good overall agreement between the theory and experiment which reveals the applicability of the boson-fermion extension of the model.

TABLE III. The subset of basis states (16) associated with the states of the GSB of odd-odd nuclei, based on $\pi h_{11/2} \otimes \nu h_{11/2}$ configuration.

| $N$ | $N_0$ | $N_0 + 2$ | $N_0 + 4$ | $N_0 + 6$ | ... |
|---|---|---|---|---|---|
| $(\lambda, \mu)$ | $(0, \mu_0)$ | $(0, \mu_0 + 1)$ | $(0, \mu_0 + 2)$ | $(0, \mu_0 + 3)$ | ... |
| $L$ | 0 | 1 | 2 | 3 | ... |
| $J$ | $I$ | $I + 1$ | $I + 2$ | $I + 3$ | ... |

To investigate the structure of the doublet bands in a certain nucleus, it is crucial to determine the $B(E2)$ and $B(M1)$ values that are very important for establishing the nature of these bands. So, in the next section we consider the $E2$ and $M1$ transitions in the framework of the orthosymplectic extension of the IVBM.

## VI. ELECTROMAGNETIC TRANSITIONS

A successful nuclear model must yield a good description not only of the energy spectrum of the nucleus but also of its electromagnetic properties. Calculation of the latter is a good test of the nuclear model functions. The most important electromagnetic features that manifest themselves in doublet bands are the $E2$ and $M1$ transitions. In this section we discuss the calculation of the $E2$ and $M1$ transition strengths between the states of the yrast band of the odd-odd nuclei based on $\pi h_{11/2} \otimes \nu h_{11/2}$ configuration and compare the results with the available experimental data.

For a mixed systems of bosons and fermions it is convenient to expand the coupled basis states (16) into the direct product of the boson and fermion states. The latter significantly simplifies the application of the Wigner-Eckart theorem in the practical calculations of the transition rates.

### A. $E2$ transitions

As was mentioned, in the symplectic extension of the IVBM the complete spectrum of the system is obtained in all the even subspaces with fixed $N$, even of the UIR $[N]_6$ of $\mathrm{U}^B(6)$, belonging to a given even UIR of $\mathrm{Sp}^B(12, R)$. The classification scheme of the $\mathrm{SU}^B(3)$ boson representations for even values of the number of bosons $N$ was presented in Table I.

In the present article, the states of the yrast band are identified with the $\mathrm{SU}^B(3)$ multiplets $(0, \mu)$. This yields the sequence $N = N_0, N_0 + 2, N_0 + 4, \ldots$ for the corresponding values $J = I, I + 1, I + 2, \ldots$ (see Table III). In terms of $(N, T)$ this corresponds to $(N = 2\mu, T = 0)$.

Using the tensorial properties of the $\mathrm{Sp}^B(12, R)$ generators with respect to (3) it is easy to define the proper $E2$ transition operator between the states of the considered band as [38]:

$$T^{E2} = e\Big[A^{[1-1]_6}_{(1,1)_3[0]_2}\ {}^{20}_{00} + \theta\big([F \times F]^{[4]_6}_{(0,2)[0]_2}\ {}^{20}_{00} + [G \times G]^{[-4]_6}_{(2,0)[0]_2}\ {}^{20}_{00}\big)\Big]. \tag{19}$$

The first part of (19) is a $\mathrm{SU}^B(3)$ generator and actually changes only the angular momentum with $\Delta L = 2$.

The tensor product

$$[F \times F]^{[4]_6}_{(0,2)[0]_2}\ {}^{20}_{00} = \sum C^{[2]_6}_{(2,0)[2]_2}\ {}^{[2]_6}_{(2,0)[2]_2}\ {}^{[4]_6}_{(0,2)[0]_2}\ C^{(2,0)\ (2,0)\ (0,2)}_{(2)_3\ (2)_3\ (2)_3} \times C^{20}_{20\ 20} C^{10}_{111-1} F^{[2]_6\ \ 20}_{(2,0)[2]_2\ \ 11} F^{[2]_6\ \ 20}_{(2,0)[2]_2\ \ 1-1} \tag{20}$$

of the operators (1) that are the pair raising $\mathrm{Sp}^B(12, R)$ generators changes the number of bosons by $\Delta N = 4$ and $\Delta L = 2$. It is obvious that this term in $T^{E2}$ (19) comes from the symplectic extension of the model. In Eq. (19) $e$ is the effective boson charge.

The transition probabilities are by definition SO(3) reduced matrix elements of transition operators $T^{E2}$ (19) between the $|i\rangle$ (initial) and $|f\rangle$ (final) collective states (16)

$$B(E2; J_i \to J_f) = \frac{1}{2J_i + 1} |\langle f \parallel T^{E2} \parallel i \rangle|^2. \tag{21}$$

The basis states (16) can be considered as a result of the coupling of the orbital $|(N, T); KLM; T_0\rangle$ (5) and spin $\phi_{Im}$ wave functions. Because the spin $I$ ($I$ − fixed) is simply added to the orbital momentum $L$, the action of the transition operator $T^{E2}$ concerns only the orbital part of the basis functions (16).

To prove the correct predictions following from our theoretical results we apply the theory to the two nuclei $^{134}$Pr and $^{132}$La for which there are available experimental data for the transition probabilities between the states of the yrast bands. The application actually consists of fitting the two parameters of the transition operator $T^{E2}$ (19) to the experiment for each of the considered bands. The $B(E2)$ strengths between the positive-parity states of the yrast band, as were attributed to the $\mathrm{SU}^B(3)$ symmetry-adapted basis states (16) of the model, are calculated. For these $\mathrm{SU}^B(3)$ multiplets, the procedure for their calculations actually coincides with that given in Ref. [38] and modified for the case of odd-odd nuclei in [46]. The theoretical predictions for the $^{134}$Pr nucleus are compared with the experimental data [29] in Fig. 10. For comparison, the IBFFM and TQPTR results (Ref. [29]) are also shown. From the figure one can see the good overall reproduction of the experimental values, which is obviously better than the IBFFM and TQPTR ones.

In Fig. 11 the theoretical predictions for the $^{132}$La nucleus are compared with the experimental data [19]. One sees that the experimental behavior of $B(E2)$ values of this nucleus is also reproduced quite well.

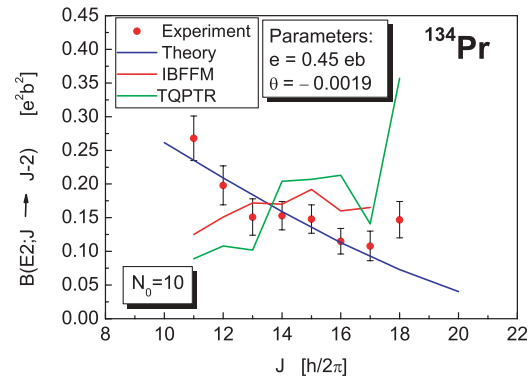


FIG. 10. (Color online) Comparison of the theoretical and experimental values for the $B(E2)$ transition probabilities for the $^{134}$Pr. The theoretical predictions of the IBFFM and TQPTR are shown as well.

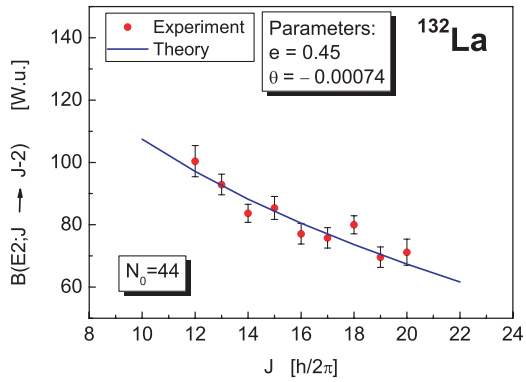


FIG. 11. (Color online) Comparison of the theoretical and experimental values for the $B(E2)$ transition probabilities for the $^{132}$La.

### B. $M1$ transitions

The structure of $M1$ transition operator between the states of the yrast band can be defined in the following way:

$$T^{M1}{}^{(1)}_{M} = \sqrt{\frac{3}{4\pi}}\Big[g J^{(1)}_M + g_{FG}\big(F_{(0,1)[0]_2}^{[2]_6\quad 1M}{}_{00} + G_{(1,0)[0]_2}^{[-2]_6\quad 1M}{}_{00}\big)\Big]. \tag{22}$$

$J^{(1)}_M$ is the total boson-fermion angular momentum, i.e., $J^{(1)}_M = L^1_M + I^{(1)}_M$, where $L^{(1)}_M = -\sqrt{2}\sum_\alpha A^1_M(\alpha,\alpha)$ and $I^{(1)}_M = [a^\dagger_j a_j]^{(1)}_M$. The second term in Eq. (22) changing the number of bosons by $\Delta N = 2$ comes also from the symplectic extension. In Eq. (22) $g$ and $g_{FG}$ stand for the gyromagnetic factors, which we consider as free parameters.

The $B(M1)$ values can be obtained from the reduced matrix elements of $M1$ operator in the usual way:

$$B(M1; J \to J') = \frac{1}{2J+1}|\langle \gamma', J' \parallel T^{M1} \parallel \gamma, J\rangle|^2. \tag{23}$$

The labels $\gamma$ and $\gamma'$ denote the quantum numbers of the basis states in chain (15).

For the calculation of the matrix element of first term in Eq. (22) we note that the $J^{(1)}_m$ operator is a generator of Spin$^{\rm BF}(3)$ algebra. Hence, the Wigner-Eckart theorem can be applied at the Spin$^{\rm BF}(3)$ level. Using the latter, one obtains for the required reduced matrix element

$$\langle \gamma', J'||J^{(1)}_m||\gamma, J\rangle = \delta_{\gamma,\gamma'}\delta_{J,J'}\sqrt{J(J+1)(2J+1)}. \tag{24}$$

Further, we will calculate the matrix element of $F_{(0,1)[0]_2}^{[2]_6\quad 10}{}_{00}$ of the second term in Eq. (22) that is a generator of Sp$^B(12, R)$ algebra. The action of the latter concerns only the orbital part of the basis functions (16). In general, for calculating the matrix elements of symplectic generators, we have the advantage of using the generalized Wigner-Eckart theorem in two steps [38]. For the SU$^B(3) \to$ SO$^B(3)$ and SU$^B(2) \to$ U$^B(1)$ reduction we need the standard SU(2) Clebsch-Gordan coefficients

$$\begin{aligned}&\langle [N'](\lambda',\mu'); K'L'M'; T'T'_0|T^{[\chi]_6\quad lm}_{[\sigma]_3[2t]_2\quad tt_0}|[N](\lambda,\mu); KLM; TT_0\rangle \\ &= \langle [N'](\lambda',\mu'); K'L'||T^{[\chi]_6\quad lm}_{[\sigma]_3[2t]_2\quad tt_0}||[N](\lambda,\mu); KL\rangle C^{L'M'}_{LMlm} C^{T'T'_0}_{TT_0tt_0}.\end{aligned} \tag{25}$$

For the calculation of the double-barred reduced matrix elements in Eq. (25) we use the next step:

$$\begin{aligned}&\langle [N'](\lambda',\mu'); K'L'||T^{[\chi]_6\quad lm}_{[\sigma]_3[2t]_2\quad tt_0}||[N](\lambda,\mu); KL\rangle \\ &= \langle [N']|||T^{[\chi]_6}_{[\sigma]_3[2t]_2}|||[N]\rangle C^{[N]_6\quad [\chi]_6\quad [N']_6}_{(\lambda,\mu)[2T]_2\quad [\sigma]_3[2t]_2\quad (\lambda',\mu')[2T']_2} \\ &\quad\times C^{(\lambda,\mu)\quad [\lambda]_3\quad (\lambda',\mu')}_{KL\quad k(l)_3\quad K'L'},\end{aligned} \tag{26}$$

where $C^{[N]_6\quad [\chi]_6\quad [N']_6}_{(\lambda,\mu)[2T]_2\quad [\sigma]_3[2t]_2\quad (\lambda',\mu')[2T']_2}$ and $C^{(\lambda,\mu)\quad [\lambda]_3\quad (\lambda',\mu')}_{KL\quad k(l)_3\quad K'L'}$ are U$^B(6)$ and SU$^B(3)$ isoscalar factors (IF's). Obviously the practical value of the application of the generalized Wigner-Eckart theorem for the calculation of the matrix elements of the Sp$^B(12, R)$ generators depends on the knowledge of the isoscalar factors for the reductions U$^B(6) \supset$ U$^B(3) \otimes$ U$^B(2)$ and U$^B(3) \supset$ O$^B(3)$, respectively. For the evaluation of the matrix elements (25) of the Sp$^B(12, R)$ operators in respect to the chain (3) the reduced triple-barred U$^B(6)$ matrix elements are also required (26).

Thus, for the calculation of the matrix element

$$\begin{aligned}&\langle [N+2], (0,\mu+1); 0L+10; 00|F_{(0,1)[0]_2}^{[2]_6\quad 10}{}_{00} \\ &\quad\times |[N], (0,\mu); 0L0; 00\rangle \\ &= C^{[N]_6\quad [2]_6\quad [N+2]_6}_{(0,\mu)[0]_2\quad (0,1)[0]_2\quad (0,\mu+1)[0]_2} C^{(0,\mu)\quad (0,1)\quad (0,\mu+1)}_{L\quad 1\quad L+1} \\ &\quad\times C^{L+1,0}_{L,0\ 1,0}\langle [N+2]|||F^{[2]_6}_{(0,1)\ [0]_2}|||[N]\rangle\end{aligned} \tag{27}$$

we use the standard recoupling technique for two coupled U$^B(6)$ tensors [38,43,47]:

$$\begin{aligned}&\langle [N']||[T^{[\alpha]_6}\times T^{[\beta]_6}]^{\sigma[\gamma]_6}|||[N]\rangle \\ &= \sum_{c,\rho_1,\rho_2} U([N]_6;[\beta]_6;[N']_6;[\alpha]_6|[N_c]_6\rho_2\rho_1;[\gamma]_6\sigma) \\ &\quad\times \langle [N']|||T^{[\alpha]_6}|||[N_c]\rangle\langle [N_c]|||T^{[\beta]_6}|||[N]\rangle,\end{aligned} \tag{28}$$

where U$(\cdots)$ are the U$^B(6)$ Racah coefficients in unitary form [48]. For the reduced triple-barred matrix element in our case, which is multiplicity free and hence there is no sum, we have

$$\begin{aligned}&\langle [N+2]|||F_{(0,1)[0]_2}^{[2]_6\quad [2]_6}|||[N]\rangle \\ &= U([N]_6;[1]_6;[N+2]_6;[1]_6|[N+1]_6;[2]_6) \\ &\quad\times \langle [N+2]|||u^{\dagger[1]_6}|||[N+1]\rangle\langle [N+1]|||u^{\dagger[1]_6}|||[N]\rangle \\ &= \sqrt{(N+1)(N+2)},\end{aligned} \tag{29}$$

where the corresponding Racah coefficient for maximal coupling representations is equal to unity [38,43,47]. For obtaining this, we used the fact that in the case of vector bosons that span the fundamental irrep [1] of $u(n)$ algebra the $u(n)$-reduced matrix element of raising generators has the well-known form [49]

$$\langle [N+1]|||u^\dagger_m(\alpha)|||[N]\rangle = \sqrt{N+1}. \tag{30}$$

Taking into account the fact that the corresponding U$^B(6)$ IF entering in Eq. (27) for maximal coupling representations is equal to 1 [38,43], we obtain

$$\begin{aligned}&\langle [N+2], (0,\mu+1); 0L+10; 00|F_{(0,1)[0]_2}^{[2]_6\quad 10}{}_{00} \\ &\quad\times |[N], (0,\mu); 0L0; 00\rangle \\ &= C^{L+1,0}_{L,0\ 1,0}\left[\frac{(\mu+L+3)(L+1)}{(\mu+1)(2L+3)}\right]^{1/2} \\ &\quad\times\sqrt{(N+1)(N+2)}.\end{aligned} \tag{31}$$

The value of the reduced $SU^B(3)$ Clebsch-Gordan coefficient (IF) is taken from Ref. [50]. Finally, the yrast condition $N = 2(\mu_0 + L) = N_0 + 2L$ (or $\mu = \mu_0 + L$) leads to the following reduced matrix element

$$\langle [N+2], (0, \mu+1); 0L+1; 00 \| F^{[2]_6 \quad 10}_{(0,1)[0]_2 \quad 00} \| [N], (0, \mu); 0L; 00 \rangle = \left[ \frac{(N_0 + 4L + 6)(L+1)}{(N_0 + 2L + 2)(2L+3)} \right]^{1/2} \times \sqrt{(N_0 + 2L + 1)(N_0 + 2L + 2)}, \quad (32)$$

where in Eq. (32) the relation $N = 2\mu + \lambda$ is taken into account. We see that the expression (32) depends on the ground state collective structure $N_0$. If $N_0 = 0$ (hence $N = 2L$), the matrix element reduces simply to

$$\langle [N+2], (0, \mu+1); 0L+1; 00 \| F^{[2]_6 \quad 10}_{(0,1)[0]_2 \quad 00} \| [N], (0, \mu); 0L; 00 \rangle = \sqrt{(2L+1)(2L+2)} \quad (33)$$

obtained in Ref. [38].

For the calculation of the matrix element of $G^{[-2]_6 \quad 10}_{(1,0)[0]_2 \quad 00}$ we use the conjugation property

$$\begin{aligned} &\langle [N-2], (0, \mu-1); 0L-1; 00 \| G^{[-2]_6 \quad 10}_{(1,0)[0]_2 \quad 00} \| [N], (0, \mu); 0L; 00 \rangle = (\langle [N], (0, \mu); 0L; 00 \| F^{[4]_6 \quad 10}_{(0,1)[0]_2 \quad 00} \| [N-2], \quad (0, \mu-1); 0L-1; 00 \rangle)^* \\ &= C^{[N-2]_6 \quad [2]_6 \quad [N]_6}_{(0,\mu-1)[0]_2 \quad (0,1)[0]_2 \quad (0,\mu)[0]_2} \times C^{(0,\mu-1) \quad (0,1) \quad (0,\mu)}_{L-1 \quad 1 \quad L} \sqrt{N(N-1)} \\ &= \left[ \frac{(N_0 + 4L + 2)L}{(N_0 + 2L)(2L+1)} \right]^{1/2} \times \sqrt{(N_0 + 2L)(N_0 + 2L - 1)}. \end{aligned} \quad (34)$$

With the help of the above analytic expressions (24), (32), and (34) one obtains the corresponding $B(M1; J \to J-1)$ values between the states in the yrast band as attributed to the $SU^B(3)$ symmetry-adapted basis states of the model (16). The numerical values obtained by fitting the two parameters $g$ and $g_{FG}$ to the experimental data for $^{134}$Pr are given in Fig. 12.

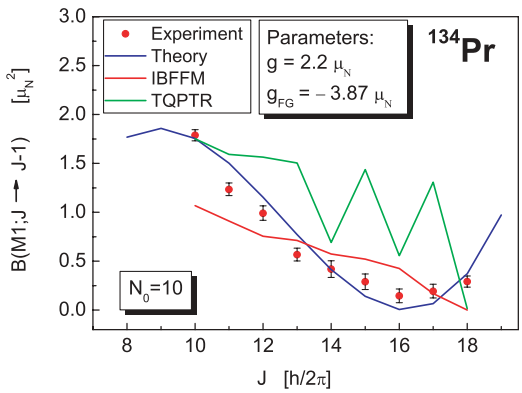


FIG. 12. (Color online) Comparison of the theoretical and experimental values for the in-band $B(M1)$ transition probabilities between the states of the yrast band for the $^{134}$Pr. The theoretical predictions of the IBFFM and TQPTR are shown as well.

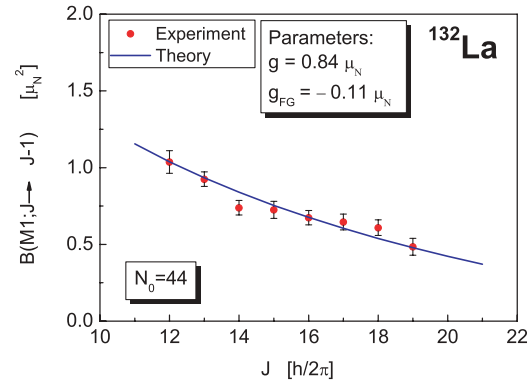


FIG. 13. (Color online) Comparison of the theoretical and experimental values for the in-band $B(M1)$ transition probabilities between the states of the yrast band for the $^{132}$La.

For comparison, the IBFFM and TQPTR results (Ref. [29]) are also shown. From the figure one can see that while the IVBM and IBFFM results in the $J \approx 13$–17 region are with almost the same level of accuracy, the general experimental trend is fairly well reproduced in the framework of the former. The adopted values of effective $g$ factors are $g = 2.2\mu_N$ and $g_{FG} = -3.87\mu_N$.

In Fig. 13 the theoretical predictions for the $^{132}$La nucleus are compared with experiment [19]. The adopted values of effective $g$ factors are $g = 0.84\mu_N$ and $g_{FG} = -0.11\mu_N$. One can observe a very good description of the experimental data within the framework of the present approach in this nucleus as well. We want to point out that the contribution of the symplectic term in Eq. (23) is crucial for the accurate reproduction of the experimental $B(M1)$ behavior.

The calculation of the $M1$ and $E2$ transitions in the sideband requires the knowledge of the corresponding $U^B(6)$ and $SU^B(3)$ isoscalar factors that are not available analytically for the basis states attributed to states of the sideband. The computer codes [51] for the numerical calculation of the $SU^B(3)$ IF's can be used, so the difficulties are focused on the calculation of the corresponding $U^B(6)$ isoscalar factors. Hence, the calculation of the transition probabilities in the sideband is a nontrivial task for a future application of our approach.

Finally, we want to point out that the expressions for the transition probabilities depend on the bandhead structure $N_0$. It turns out that the values of $B(E2)$ and $B(M1)$ transition strengths are very sensitive to the initial number of bosons $N_0$. Usually, the bandhead structures of the GSB of the even-even core and the yrast band of the doubly odd (or odd-mass) nuclei are different. This suggests modified values of the effective charges and gyromagnetic factors required for the calculation of the $B(E2)$ and $B(M1)$ transition probabilities in the neighboring even-even and odd-$A$ nuclei.

## VII. CONCLUSIONS

In the present article, the yrast and yrare states with the $\pi h_{11/2} \otimes \nu h_{11/2}$ configuration in the doubly odd nuclei, $^{126}$Pr, $^{134}$Pr, and $^{132}$La, were investigated in terms of the

orthosymplectic extension of the IVBM. This allows for the proper reproduction of the energies of these states up to high angular momenta in both bands.

The basis states of the odd-mass and odd-odd systems are classified by the dynamical symmetry (15) and the model Hamiltonian is written in terms of the first- and second-order invariants of the groups from the corresponding reduction chain. Hence the problem is exactly solvable within the framework of the IVBM that, in turn, yields a simple and straightforward application to real nuclear systems.

For two of the three isotopes considered, the $B(E2)$ and $B(M1)$ transition probabilities between the states of the yrast band are calculated and compared with the experimental data. A good overall agreement of the theoretical predictions with experiment is obtained. The calculations reveal the important role of the symplectic term entering in the corresponding transition operator for the correct reproduction of the behavior of both $B(E2)$ and $B(M1)$ strengths.

The even-even nuclei are used as a core on which the collective excitations of the neighboring odd-mass and odd-odd nuclei are built on. Thus, the spectra of odd-mass and odd-odd nuclei arise as a result of the coupling of the fermion degrees of freedom to the boson core. The states of the yrast band of doubly odd nuclei are built on the ground state band $\mathrm{SU}^B(3)$ multiplets $(0, \mu)$ of the even-even core, while those of sideband are built on the $\mathrm{SU}^B(3)$ multiplets $(\lambda_0 = \text{fixed}, \mu)$ that suggests similar collective behavior [both sets of $\mathrm{SU}^B(3)$ multiplets are the stretched states of second type] of the two bands. The only difference comes from the initial band head structures [$(0, \mu)$ and $(\lambda_0, \mu)$]. Hence, a purely collective structure of the states of the yrast and sidebands is introduced. Those assumptions suggest a similar behavior (slope) of the transitions in the sideband that we intend to investigate in future.

The good agreement between the theoretical and the experimental band structures is a result of the mixing of the basic collective modes—rotational and vibrational ones arising from the yrast conditions—way back on the level of the even-even cores. This allows for the correct reproduction of the high-spin states of the collective bands and the correct placement of the different bandheads. The simplifications in our approach comes from the fact that only one dynamical symmetry is employed, which leads to exact and simple solutions depending only on the values of the model parameters. The success of the presented applications is based on the proper and consistent mapping of the experimentally observed collective states of the even-even, odd-mass, and odd-odd nuclei on the (ortho-)symplectic structures. The latter is much simpler approach than the mixing of the basis states considered in other theoretical models.

The presented results on the description of the doublet bands in odd-odd nuclei confirm the wider applicability of the used boson-fermion symmetry of IVBM.

## ACKNOWLEDGMENTS

This work was supported by the Bulgarian National Foundation for scientific research under grant number Φ-1501. H.G.G. acknowledges also the support from the European Operational programm HRD through contract BG051PO001/07/3.3-02 with the Bulgarian Ministry of Education.

[1] K. Starosta *et al.*, Phys. Rev. Lett. **86**, 971 (2001).
[2] A. A. Hecht *et al.*, Phys. Rev. C **63**, 051302(R) (2001).
[3] T. Koike *et al.*, Phys. Rev. C **63**, 061304(R) (2001).
[4] D. J. Hartley *et al.*, Phys. Rev. C **64**, 031304(R) (2001).
[5] R. A. Bark *et al.*, Nucl. Phys. **A691**, 577 (2001).
[6] K. Starosta *et al.*, Phys. Rev. C **65**, 044328 (2002).
[7] T. Koike, K. Starosta, C. J. Chiara, D. B. Fossan, and D. R. LaFosse, Phys. Rev. C **67**, 044319 (2003).
[8] G. Rainovski *et al.*, Phys. Rev. C **68**, 024318 (2003).
[9] S. Frauendorf and J. Meng, Nucl. Phys. **A617**, 131 (1997).
[10] K. Starosta *et al.*, Phys. Rev. Lett. **86**, 971 (2001).
[11] A. A. Hecht *et al.*, Phys. Rev. C **63**, 051302(R) (2001).
[12] V. I. Dimitrov, S. Frauendorf, and F. Donau, Phys. Rev. Lett. **84**, 5732 (2000).
[13] A. J. Simons *et al.*, J. Phys. G: Nucl. Part. Phys. **31**, 541 (2005).
[14] R. A. Bark *et al.*, Nucl. Phys. **A691**, 577 (2001).
[15] T. Koike, K. Starosta, and I. Hamamoto, Phys. Rev. Lett. **93**, 172502 (2004).
[16] I. Ragnarsson and P. Semmes, Hyperfine Interact. **43**, 423 (1988).
[17] S. Brant, D. Vretenar, and A. Ventura, Phys. Rev. C **69**, 017304 (2004).
[18] E. Grodner, J. Srebrny, Ch. Droste, T. Morek, A. Paster-nak, J. Kownacki, Int. J. Mod. Phys. E **13**, 243 (2004).
[19] J. Srebrny *et al.*, Acta Phys. Pol. B **36**, 1063 (2005).
[20] D. Tonev *et al.*, Phys. Rev. Lett. **96**, 052501 (2006).
[21] C. M. Petrache, G. B. Hagemann, I. Hamamoto, and K. Starosta, Phys. Rev. Lett. **96**, 112502 (2006).
[22] K. Higashiyama and N. Yoshinaga, Prog. Theor. Phys. **113**, 1139 (2005).
[23] K. Higashiyama, N. Yoshinaga, and K. Tanabe, Phys. Rev. C **72**, 024315 (2005).
[24] N. Yoshinaga and K. Higashiyama, J. Phys. G: Nucl. Part. Phys. **31**, S1455 (2005).
[25] N. Yoshinaga and K. Higashiyama, Eur. Phys. J. A **30**, 343 (2006); **31**, 395 (2007).
[26] K. Higashiyama and N. Yoshinaga, Eur. Phys. J. A **33**, 355 (2007).
[27] V. Paar, *Capture Gamma-Ray Spectroscopy and Related Topics*, edited by S. Raman, AIP Conf. Proc. No. 125 (AIP, New York, 1985), p. 70; S. Brant, V. Paar, and D. Vretenar, Z. Phys. A **319**, 355 (1984); V. Paar, D. K. Sunko, and D. Vretenar, Z. Phys. A **327**, 291 (1987).
[28] S. Brant and V. Paar, Z. Phys. A **329**, 151 (1988).
[29] D. Tonev *et al.*, Phys. Rev. C **76**, 044313 (2007).
[30] S. Brant, D. Tonev, G. de Angelis, and A. Ventura, Phys. Rev. C **78**, 034301 (2008).
[31] C. M. Petrache *et al.*, Phys. Rev. C **64**, 044303 (2001).
[32] H. Ganev, V. P. Garistov, and A. I. Georgieva, Phys. Rev. C **69**, 014305 (2004).
[33] H. G. Ganev, J. Phys. G: Nucl. Part. Phys. **35**, 125101 (2008).

[34] H. G. Ganev and A. I. Georgieva, *Boson and fermion degrees of freedom in orthosympletic extension of the IVBM: odd-odd nuclear spectra*, in *Proceedings of the XXVII International Workshop on Nuclear Theory (June 23–28, 2008, Rila Mountains, Bulgaria)*, edited by S. Dimitrova (BM Trade Ltd., Sofia, Bulgaria, 2008), pp. 155–167.
[35] A. Georgieva, P. Raychev, and R. Roussev, J. Phys. G: Nucl. Part. Phys. **8**, 1377 (1982).
[36] C. Quesne, J. Math. Phys. **14**, 366 (1973).
[37] D. J. Rowe, Rep. Prog. Phys. **48**, 1419 (1985).
[38] H. G. Ganev and A. I. Georgieva, Phys. Rev. C **76**, 054322 (2007).
[39] H. G. Ganev, V. P. Garistov, A. I. Georgieva, and J. P. Draayer, Phys. Rev. C **70**, 054317 (2004).
[40] Evaluated Nuclear Structure Data File (ENSDF), http://ie.lbl.gov/databases/ensdfserve.html.
[41] L. Wilets and M. Jean, Phys. Rev. **102**, 788 (1956).
[42] C. M. Petrache, S. Brant, D. Bazzacco, G. Falconi, E. Farnea, S. Lunardi, V. Paar, Zs. Podolyak, R. Ventureli, and D. Vretenar, Nucl. Phys. **A635**, 361 (1998).
[43] B. G. Wybourne, *Classical Groups for Physicists* (Wiley, New York, 1974).
[44] G. Rosensteel and D. J. Rowe, Phys. Rev. C **67**, 014303 (2003).
[45] J. P. Elliott, Proc. R. Soc. London A **245**, 562 (1958).
[46] H. G. Ganev (unpublished).
[47] C. Quesne, J. Phys. A: Math. Gen. **23**, 847 (1990); **24**, 2697 (1991).
[48] K. T. Hecht, R. Le Blanc, and D. J. Rowe, J. Phys. A: Math. Gen. **20**, 2241 (1987).
[49] R. Le Blanc and D. J. Rowe, J. Phys. A: Math. Gen. **20**, L681 (1987).
[50] J. D. Vergados, Nucl. Phys. **A111**, 681 (1968).
[51] J. P. Draayer and Y. Akiyama, J. Math. Phys. **14**, 1904 (1973); Y. Akiyama and J. P. Draayer, Comput. Phys. Commun. **5**, 405 (1973); C. Bahri and J. P. Draayer, Comput. Phys. Commun. **83**, 59 (1994); C. Bahri, D. J. Rowe, and J. P. Draayer, Comput. Phys. Commun. **159**, 121 (2004).